Low apparent activation energy of ammonia synthesis over Ru catalyst supported by hydrogen storage material

Ryusei Morimoto[1,†], Takaya Ogawa[2,†,], Kazuma Torii[2], Tetsu Seno[2], Hideyuki Okumura[2], Keiichi N. Ishihara[2]*

[1]*Undergraduate school of chemical science and technology, Faculty of Engineering, Kyoto University, Yoshida-Honmachi, Sakyo-ku, Kyoto 606-8501, Kyoto 606-8501, Japan*

E-mail address: morimoto.ryusei.86c@st.kyoto-u.ac.jp (R. M.)

[2]*Department of Socio-Environmental Energy Science, Graduate School of Energy Science, Kyoto University, Yoshida-Honmachi, Sakyo-ku, Kyoto Sakyo-ku, Kyoto 606-8501, Japan*

**Corresponding author. E-mail address: ogawa.takaya.8s@kyoto-u.ac.jp (T. O.)*

Abstract

Ruthenium is an excellent catalyst for ammonia synthesis and recently shows quite high activity when supported on materials with high electron-donating and hydrogen-absorbing properties. The high activity is generally considered to originate from the two effects: the electron-donating property of the support, which reduces its apparent activation energy ($^{app}E_a$) to half of pure Ru's $^{app}E_a$, and the hydrogen-absorbing property, which increases the active site by suppressing hydrogen poisoning, a drawback of ruthenium catalysts. Here, we investigated the catalytic performance of ruthenium loaded on $TiMn_2$ and ZrH_2, hydrogen storage materials without electron-donating property to ruthenium. Ruthenium on $TiMn_2$ and ZrH_2 showed the $^{app}E_a$ reduced by half despite the lack of electron-donating property. It is plausible that the decreased $^{app}E_a$ is due to the elimination of hydrogen over Ru by $TiMn_2$ and ZrH_2. The hydrogen storage capacity is also an essential factor in discussing the $^{app}E_a$.

Introduction

Ammonia is indispensable for human beings as an artificial fertilizer and is one of the most produced chemicals. The amount of ammonia production is more than 182 million tonnes in 2019 and is expected to increase by 4% during the next four years[1]. Ammonia has been industrially synthesized at 400−500 °C and 10−30 MPa using an Fe-based catalyst for over 100 years[2,3]. However, these severe conditions require a large, robust, and expensive plant. Therefore, the business model is the synthesis at a large scale and distribution ammonia to each area. It results in scarce fertilizer in many countries that do not have sufficient transport infrastructures, such as Zambia, Tanzania, Ghana, and Nigeria[4]. The milder reaction condition would realize ammonia synthesis at a small scale and supply ammonia to local agricultural lands, making the fertilizer cost affordable, increasing food production, and reducing starvation.

Ru has been known to synthesize ammonia with high activity when the electropositive metal is added, although the fatal drawback of Ru is hydrogen poisoning[3,5–8]. It was recently reported that Ru supported on oxyhydride- and oxynitride-based materials are highly reactive even under mild conditions[9–14]. For example, Ru supported on electride $[Ca_{24}Al_{28}O_{64}]^{4+}(e^-)_4$ (Ru/C12A7:e^-) shows high reactivity,[15] where C12A7:e^- has two characteristic properties: one is the hydrogen storage capacity, which suppresses hydrogen poisoning and increases the number of

active Ru sites. The other is the high electron-donating property, which reduces the apparent activation energy ($^{app}E_a$) to half of Ru bulk's $^{app}E_a$ and enhances the reaction rate. There are many reports similar to this, and electron-donating properties are generally considered an important factor in lowering $^{app}E_a$.

Meanwhile, the coverage of hydrogen and nitrogen has a dependency on temperature[16]. For example, with the adsorption-desorption reaction of species A given by

$$A + * \rightleftharpoons A^* \quad (1)$$

Where * means an unoccupied site. We can associate the reaction fraction, $\theta_A/p_A\theta_*$, where θ_A is a fractional coverage of the adsorbate A on the surface, P_A is a pressure of gas A, and a probability that a site is unoccupied, θ_*. At equilibrium, we have

$$\left.\frac{\theta_A}{P_A\theta_*}\right|_{Eq} = K_{ads} = e^{-\frac{\Delta G_{ads}}{k_B T}} \quad (2)$$

where K_{ads} is an equilibrium constant of the adsorption, ΔG_{ads} is the change of Gibbs free energy by the adsorption of A, k_B is Boltzmann constant, and T is temperature. Then, the coverage depends on temperature and directly determines reaction rates. In the case that the rate-determining step is the reaction, $A^* + B^* \rightarrow AB^{*+*}$, a reaction rate, r_{AB}, is described as follows

$$r_{AB} = k_{AB}\theta_A\theta_B \quad (3)$$

where k_{AB} is a reaction constant for the reaction. Therefore, $^{app}E_a$, estimated by the temperature dependence of k_{AB}, is influenced by the coverage through the equation below:

$$^{app}E_a = -\frac{d(lnr_{AB})}{d\left(1/k_BT\right)} = -\frac{d(lnk_{AB} + ln\theta_A + ln\theta_B)}{d\left(1/k_BT\right)} = E_a - \frac{d(ln\theta_A + ln\theta_B)}{d\left(1/k_BT\right)} \quad (4)$$

As well as the assumed reaction, the hydrogen storage ability itself can change θ_H, increasing the coverage of other species and changing the $^{app}E_a$. However, the influence of hydrogen storage ability on $^{app}E_a$ has not been discussed for the recent catalysts.

In this paper, we prepared Ru on hydrogen storage material, $TiMn_2$ and ZrH_2. The work functions of Ti, Mn, Zr, and Ru are 4.3, 4.1, 4.1, and 4.7 eV, respectively, which are or similar values and hardly donates an electron to Ru from $TiMn_2$ and ZrH_2. Thus, the function of only hydrogen storage ability on $^{app}E_a$ can be estimated. The 1−10wt% of Ru on $TiMn_2$ and ZrH_2 catalysts were prepared to demonstrate the influence of the $Ru/TiMn_2$ and Ru/ZrH_2 ratio. For comparisons, Ru bulk and Ru dispersed on carbon and MgO were investigated. To discuss the effect of electron donation to Ru on $^{app}E_a$, K was added as an electropositive metal.

Experimental methods

The preparation of catalysts The powder of $TiMn_2$ (Mn:~51%, Ti:~29%, V:~14%, Fe, Cr, Zr: ~6%, Sigma-Aldrich Co. LLC) was prepared by only hand milling with an alumina mortar and pestle. ZrH_2 (Zr + Hf:97.6 %, H:2.1%, Mitsuwa Chemicals) was prepared in the same manner of $TiMn_2$. The work function of V, Fe, Cr, and Zr are 4.3, 4.5, 4.5, and 4.1 eV, respectively, and are considered not to donate electrons to Ru. Ruthenium (III) acetylacetonate ($Ru(acac)_3$, Strem Chemicals, Inc) was dissolved in tetrahydrofuran (THF, ≥99.5%, Fujifilm Wako Pure Chemical Corporation). The $TiMn_2$ and ZrH_2 powder was dispersed in the solution and evaporated in a vacuum at elevated temperature with staring. The amount of loaded Ru was 1, 3, 5 10 wt% (Xwt%$Ru/TiMn_2$ or Xwt%Ru/ZrH_2 when Xwt% of Ru was loaded). 1wt% Ru on MgO (99.9%, Kojundo Chemical Lab. Co., Ltd., 1wt%Ru/MgO) and 10 wt% Ru on carbon (99.9%, Kojundo Chemical Lab. Co., Ltd., 10wt%Ru/C) were prepared in the same way using

$Ru(acac)_3$, where MgO and C were employed not to have electron donation and hydrogen storage properties. K was added to $Ru/TiMn_2$, Ru/ZrH_2, or Ru using KNO_3 aqueous solution (99.9%, Fujifilm Wako Pure Chemical Corporation) and evaporated in a vacuum at elevated temperature with staring, adjusting the ratio of Ru and K to 1:1 ($Ru\text{-}K/ZrH_2$, Ru+K, respectively). K was added to the ZrH_2 powder, in the same way, adjusting the K and ZrH_2 ratio to the same with $7wt\%Ru+K/ZrH_2$. For a comparison, Ru powder (Ru bulk, ≤0.3μm (TRU-300), Tokuriki-Honten CO. LTD) was tested as purchased.

The catalysts characterization. The Brunauer−Emmett−Teller (BET) specific surface areas of the samples were determined from nitrogen adsorption−desorption isotherms measured at −196 °C using an automatic gas-adsorption instrument: (Tristar II plus, Micromeritics). X-ray diffraction (XRD) patterns were obtained (RINT2100CMJ, Rigaku). Temperature programmed H_2-desorption (H_2-TPD) was performed under Ar flow (30 mL min^{-1}), 298~873 K, using an instrument (AutoChem II 2920, micromeritics). CO chemisorption was measured using same instrument as H_2-TPD.

The characterization of catalytic activity. The reactivities of the catalysts were demonstrated in a stainless-steel flow set-up. Supplied gas is an extrapure (99.9999 %) mixture of H_2, N_2, and Ar. Before the reactions, all the catalysts were treated in a stream of N_2:H_2 =1:3 under 0.1 MPa, raising reaction temperature by 200 °C h^{-1}. The temperature range of ${}^{app}E_a$ measurement was 380−460 °C. The concentration of ammonia in the stream that left the catalyst bed was monitored under steady-state temperature conditions. The ammonia produced was trapped in 5 mM H_2SO_4. The amount of NH_4^+ in the solution was determined using an ion chromatograph (Eco IC, Metrohm) equipped with a conductivity detector.

Kinetic Analysis The reaction orders of $N_2(\alpha)$, $H_2(\beta)$, and $NH_3(\gamma)$ was determined by changing the flow ratio of H_2, N_2, and Ar in the similar way with previous publication[17] with the equation below.

$$r = kP_{N_2}{}^{\alpha} P_{H_2}{}^{\beta} P_{NH_3}{}^{\gamma} \quad (5)$$

The analysis was conducted at 0.1 MPa and 440 °C. RDS (rate-determining step) was determined in similar way with previous studies[18].

Results

The catalytic activities for ammonia synthesis were summarized in Table 1. The $Ru/TiMn_2$ and Ru/ZrH_2 showed the reduced ${}^{app}E_a$, mostly the half of Ru bulk's ${}^{app}E_a$. $TiMn_2$ and ZrH_2 without Ru exhibited negligible activity. In addition, 10wt%Ru/C did not possess such low ${}^{app}E_a$. Hence, the combination of $TiMn_2$, ZrH_2 and Ru causes the low ${}^{app}E_a$. Although the amount of ammonia synthesis increased as the amount of Ru loaded on TiMn2 and ZrH2 increased, the ${}^{app}E_a$ did not change significantly. It should be reasonable that a low ${}^{app}E_a$ does not result in a high reaction rate.

Table 1. Catalytic performance of Ru catalysts for ammonia synthesis.

catalyst	Ru-loading (wt%)	Surface area (m^2 g^{-1})	NH_3 formation (μmol g^{-1} h^{-1})[a]	E_a (kJ mol^{-1})[b]
Ru	-	4.38	531.0	118.0
K/Ru	-	4.75	1918.4	111.5
$TiMn_2$	-	0.36	negligible	-
Ru/$TiMn_2$	1		9.7	79.7
	10		43.8	64.5
Ru/C	10		6.3	110.5
ZrH_2	-	0.44	negligible	-
Ru/ZrH_2	1		55.8	72.5
	5		476.1	61.8
	7	0.51	573.6	70.3
	10		181.3	65.5
Ru-0.2K/ZrH_2	7		698.3	64.5

[a]The catalytic activities at 0.1 MPa and 400 °C with N_2:H_2 =1:3 under 0.1 MPa. [b]The temperature range of measurement is 380−460 °C.

When K was added to Ru and Ru/ZrH_2 catalysts, the activities of both catalysts were enhanced. For 7wt%Ru-0.2K/ZrH_2, the improved activity is attributed to the enlarged surface area, although the $^{app}E_a$ decreased. Ru+K showed the highest activity among the catalysts tested in this paper even though $^{app}E_a$ is not the lowest. It is the same conclusion as the previous paragraph.

Table 2. Reaction orders of catalysts.

catalyst	N_2 order (α)	H_2 order (β)	NH_3 order (γ)
Ru bulk	0.92	-0.65	-0.15
10wt%Ru/$TiMn_2$	1.22	1.13	-1.06
1wt%Ru/ZrH_2	0.79	0.74	-0.65
7wt%Ru/ZrH_2	1.63	0.98	-1.70
7wt%Ru-0.2K/ZrH2	0.75	0.31	-0.26

Table 2 shows the reaction orders of Ru bulk, 10wt%Ru/$TiMn_2$, 1wt%Ru/ZrH_2, 7wt%Ru/ZrH_2, and 7wt%Ru-0.2K/ZrH_2. As we expected, the reaction order for hydrogen over Ru/ZrH_2 and Ru/$TiMn_2$ was positive, which means $TiMn_2$ and ZrH_2 successfully suppressed hydrogen poisoning. On the other hand, $TiMn_2$ and ZrH_2 have more negative ammonia order than Ru bulk, which makes them more susceptible to ammonia poisoning. The addition of K on ZrH_2 resulted in more positive for ammonia order and more negative for the hydrogen order. Therefore, the

addition of K can change the active sites of catalysts.

The hydrogen storage capacity over ZrH_2 and $TiMn_2$ was investigated using H_2-TPD method under Ar flow. Figure 1 shows H_2-TPD results of ZrH2, 7wt%Ru/ZrH2, and 7wt%Ru-0.2K/ZrH2. ZrH_2 released hydrogen from around 400 ℃, but Ru/ZrH_2 released from around 150 ℃. The addition of Ru facilitates the release of hydrogen at lower temperatures and improves the activity of ammonia synthesis at low temperatures. $Ru\text{-}0.2K/ZrH_2$ released less hydrogen than Ru/ZrH_2 at the temperatures where ammonia synthesis took place (380~460°C). $Ru\text{-}0.2K/ZrH_2$ released less hydrogen than Ru/ZrH_2 at the temperatures where ammonia synthesis was carried out (380~460 °C), consistent with $Ru\text{-}0.2K/ZrH_2$ being more susceptible to hydrogen poisoning.

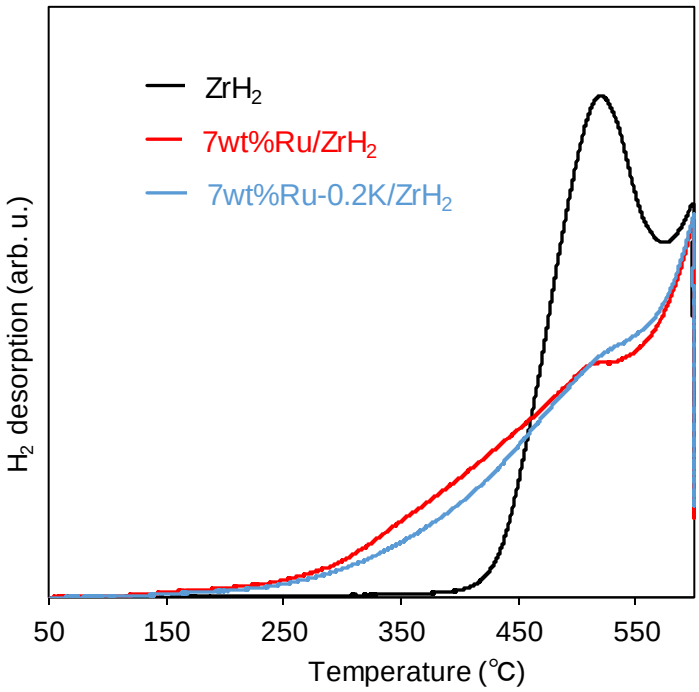

Figure 1. H_2-TPD profiles of ZrH_2, 7wt%Ru/ZrH_2, and 7wt%$Ru\text{-}0.2K/ZrH_2$.

Figure 2 shows H_2-TPD results of $TiMn_2$ and 1wt%$Ru/TiMn_2$. $TiMn_2$ begins to release hydrogen at around 250 °C, while $Ru/TiMn_2$ begins to release hydrogen at around 150 °C. Similar to ZrH_2, the addition of Ru to $TiMn_2$ also facilitated the release of hydrogen at lower temperatures.

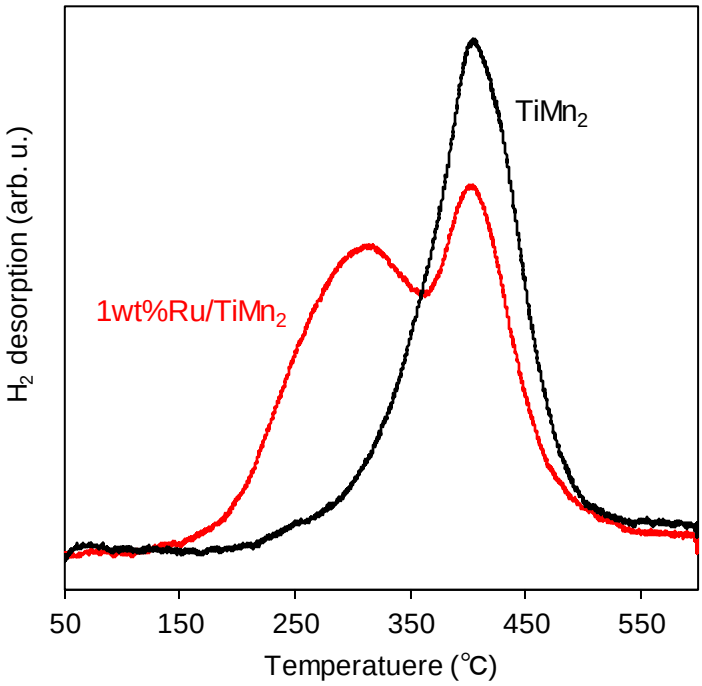

Figure 2. H_2-TPD profiles of $TiMn_2$ and 1wt%Ru/$TiMn_2$.

The value of Ru dispersion was 26.9% and the size of Ru particles 4.81 nm for 1wt%Ru/ZrH_2 measured by CO chemisorption.

The RDS of 10wt%Ru/$TiMn_2$ and 7wt%Ru/ZrH_2 were investigated using the least-square method in the same way of previous study[18]. Figure 4 shows the fitting result of 7wt%Ru/ZrH2. The R^2 value was 0.907 when step 6 was assumed to be RDS and the highest, and RDS of 7wt%Ru/ZrH_2 becomes step 6.

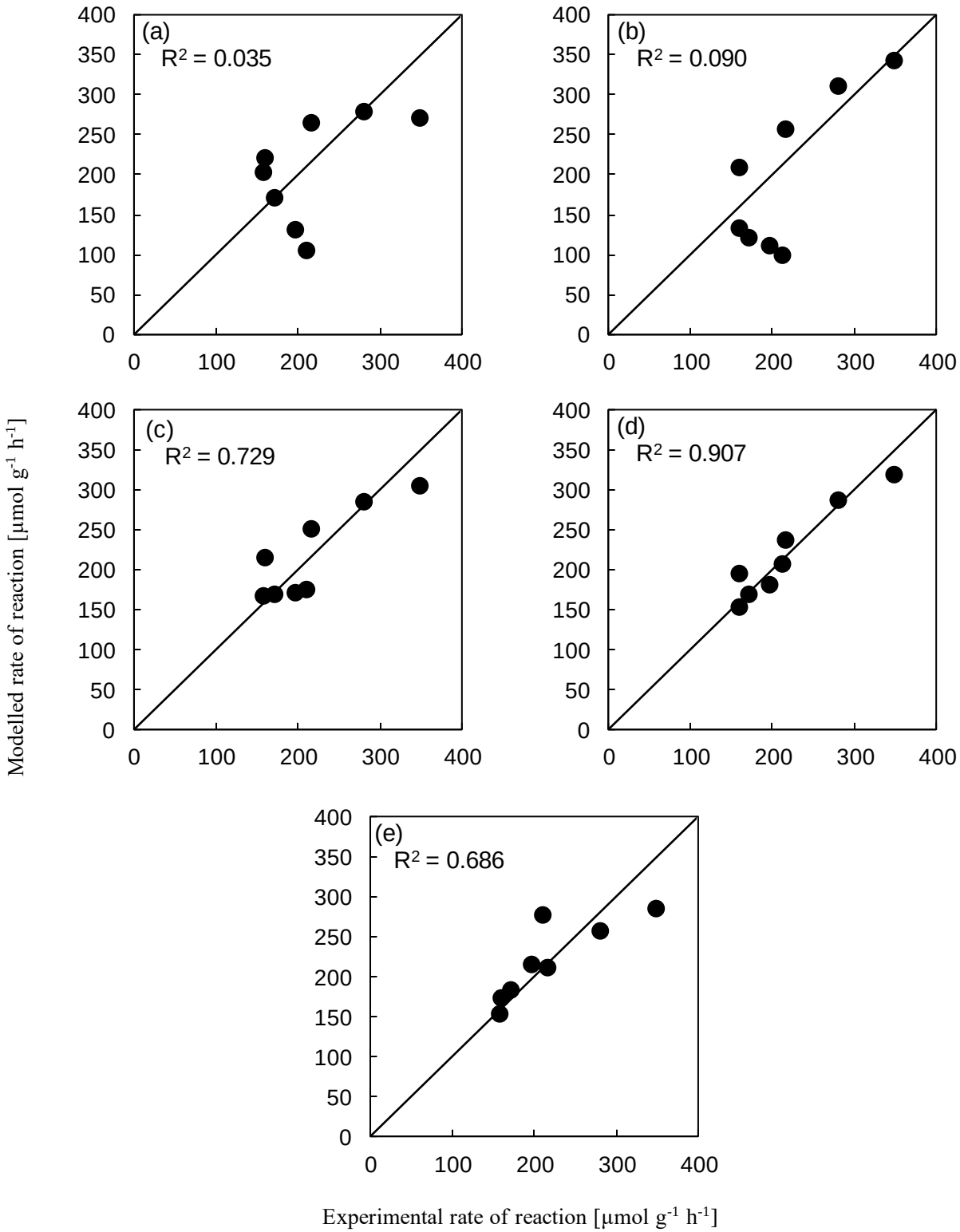

Figure 3. Comparison of experimental and calculated reaction rates at 440 ℃ over 7wt%Ru/ZrH_2 with respect to the rate equations derived with the RDS assumed to be (a) step 3 [$N_2 * \rightarrow 2N *$], (b) step 4 [$N * + H * \rightleftharpoons NH * + *$], (c) step 5 [$NH * + H * \rightleftharpoons NH_2 * + *$], (d) step 6 [$NH_2 * + H * \rightleftharpoons NH_3 * + *$], (e) step7 [$NH_3 * \rightleftharpoons NH_3 + *$].

Figure 4 shows the fitting result of 10wt%Ru/TiMn2. When step 6 was assumed to be RDS, the R^2 value of 10wt%Ru/$TiMn_2$ was 0.971, which was the highest among steps 3-7. Therefore, step 6 was RDS as well as 7wt%Ru/ZrH_2. Although the RDS of conventional ruthenium catalysts such as Ru and Ru/MgO was nitrogen dissociation (step 3)[18,19], the Ru/ZrH_2 and Ru/$TiMn_2$ used in this study were found to be NH_3* formation reactions

(step 6).

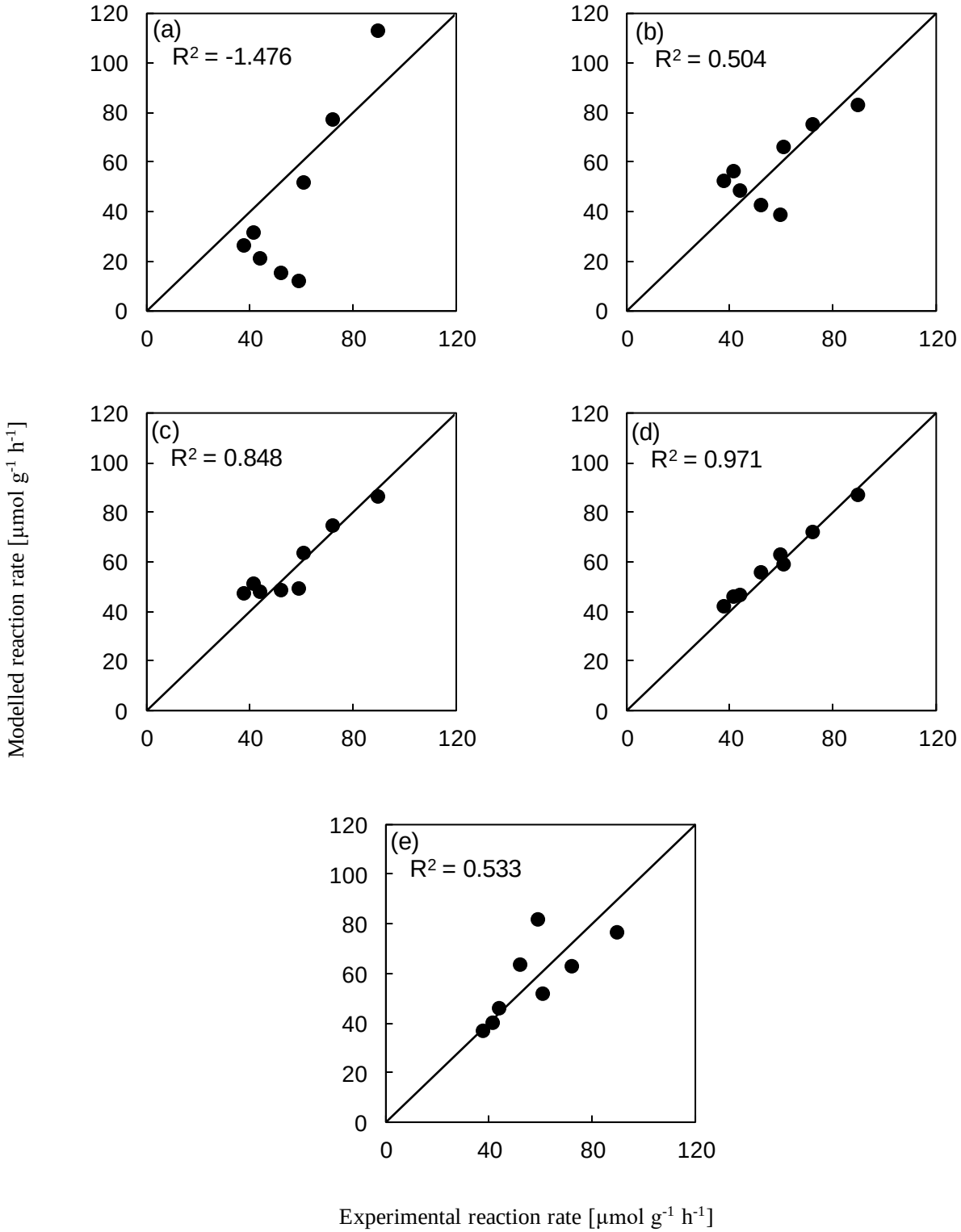

Figure 4. Comparison of experimental and calculated reaction rates at 440 °C over 10wt%Ru/$TiMn_2$ with respect to the rate equations derived with the RDS assumed to be (a) step 3 [$N_2 * \rightarrow 2N *$], (b) step 4 [$N * + H * \rightleftharpoons NH * + *$], (c) step 5 [$NH * + H * \rightleftharpoons NH_2 * + *$], (d) step 6 [$NH_2 * + H * \rightleftharpoons NH_3 * + *$], (e) step7 [$NH_3 * \rightleftharpoons NH_3 + *$].

Discussion

Eq. (2) indicates that θ_H decreases when the temperature is elevated, eliminating hydrogen poisoning and increasing θ_N. The large θ_N enhances reaction rate as well as Eq. (3), which leads to a high dependency of reaction

rate on temperature. The reaction order of 10wt%Ru/$TiMn_2$ and 7wt%Ru/ZrH_2 was positive, and thus the hydrogen poisoning over the Ru supported by $TiMn_2$ and ZrH_2 was overcome. It can be interpreted that the θ_H was reduced not by temperature but by the hydrogen storage material. Then, the dependence on temperature of reaction rate was mitigated, which can result in low $^{app}E_a$. In fact, the $^{app}E_a$s of Ru/$TiMn_2$ and Ru/ZrH_2 catalysts decreased to almost half of the Ru bulk's $^{app}E_a$. The lower $^{app}E_a$ can be explained by the hydrogen storage ability of support materials.

The density functional theory (DFT) calculation indicates the E_a for ammonia synthesis over Ru without electron donation is around 100 kJ/mol, which is higher than the $^{app}E_a$s of the tested catalysts. It is possible that over Ru supported on hydrogen storage materials, θ_* is dominant rather than θ_H and θ_N. Therefore, the raised temperature induces both lower θ_H and θ_N, which slowdowns r and mitigates the temperature dependency of reaction rate. It can decrease the $^{app}E_a$ than the actual E_a.

The addition of Ru nanoparticles to hydrogen storage alloys lowers the temperature at which they begin to absorb and release hydrogen by 100~250 ℃, suggesting that the addition of ruthenium may enable ammonia synthesis at lower temperatures in other hydrogen storage alloys that release hydrogen at higher temperatures than the conditions for ammonia synthesis.

The hydrogen poisoning over Ru+K was suppressed, as shown by the reaction order of hydrogen over Ru+K. In addition, the 7wt%Ru-0.2K/ZrH_2 exhibits the less $^{app}E_a$ than that of 7wt%Ru/ZrH_2. Then, the reduced $^{app}E_a$ of Ru+K can be explained by electron donation from K and storing hydrogen. It would be concluded that both electron-donating and hydrogen storage properties have an enormous influence on an $^{app}E_a$. According to the XANES spectrum in the previous report[20], the K-edge of Ru on C12A7:e^- did not shift to lower energy, which means electrons were not donated to Ru from C12A7:e^- although the N≡N bonding on Ru/C12A7:e^- is weakened at −170°C under 5 kPa of N_2 [15]. The $^{app}E_a$ of Ru/C12A7:e^- is around 40 kJ/mol at the lowest, similar to the $^{app}E_a$ of 1wt%Ru/$TiMn_2$. Recent progress of catalysts associated with much-reduced $^{app}E_a$ of ammonia synthesis might be explained by the influence of the hydrogen storage ability.

Conclusion

The catalytic performance of ammonia synthesis over Ru supported by hydrogen storage alloy, $TiMn_2$ and ZrH_2, was examined to estimate the influence of only hydrogen storage property on $^{app}E_a$. The positive reaction orders of hydrogen on Ru/$TiMn_2$ and Ru/ZrH_2 indicate that the hydrogen poisoning over the Ru on $TiMn_2$ and ZrH_2 is suppressed. Ru/$TiMn_2$ and Ru/ZrH_2 catalysts exhibit low $^{app}E_a$, almost half of Ru bulk's $^{app}E_a$. The decreased θ_Hs over Ru derived from hydrogen storage properties are considered to reduce their $^{app}E_a$. Besides, even if the $^{app}E_a$ is not low, the reaction rate can be high according to the results of Ru/$TiMn_2$ and Ru+K. Hydrogen storage properties should be included to discuss reduced $^{app}E_a$, which would give the correct direction to design a new catalyst of ammonia synthesis.

Acknowledgment

This research was supported by the Environment Research and Technology Development Fund (JPMEERF20192R02) of the Environmental Restoration and Conservation Agency of Japan (ERCA), and Precursory Research for Embryonic Science and Technology (PRESTO, JPMJPR2273) of the Japan Science and Technology Agency (JST).

Reference

(1) *Mineral Commodity Summaries 2022*; U. S. Geological Survey, 2022. https://doi.org/10.3133/mcs2022.

(2) Liu, H. Ammonia Synthesis Catalyst 100 Years: Practice, Enlightenment and Challenge. *Chin. J. Catal.* **2014**, *35* (10), 1619–1640. https://doi.org/10.1016/S1872-2067(14)60118-2.

(3) Liu, H. *Ammonia Synthesis Catalysts: Innovation and Practice*; WORLD SCIENTIFIC / CHEMICAL INDUSTRY PRESS, CHINA, 2013. https://doi.org/10.1142/8199.

(4) Morris, M.; Kelly, V. A.; Kopicki, R. J.; Byerlee, D. *Fertilizer Use in African Agriculture: Lessons Learned and Good Practice Guidelines*; The World Bank, 2007. https://doi.org/10.1596/978-0-8213-6880-0.

(5) Aika, K.; Hori, H.; Ozaki, A. Activation of Nitrogen by Alkali Metal Promoted Transition Metal I. Ammonia Synthesis over Ruthenium Promoted by Alkali Metal. *J. Catal.* **1972**, *27* (3), 424–431. https://doi.org/10.1016/0021-9517(72)90179-0.

(6) Saadatjou, N.; Jafari, A.; Sahebdelfar, S. Ruthenium Nanocatalysts for Ammonia Synthesis: A Review. *Chem. Eng. Commun.* **2015**, *202* (4), 420–448. https://doi.org/10.1080/00986445.2014.923995.

(7) Aika, K. Role of Alkali Promoter in Ammonia Synthesis over Ruthenium Catalysts—Effect on Reaction Mechanism. *Catal. Today* **2017**, *286*, 14–20. https://doi.org/10.1016/j.cattod.2016.08.012.

(8) Ogawa, T.; Kobayashi, Y.; Mizoguchi, H.; Kitano, M.; Abe, H.; Tada, T.; Toda, Y.; Niwa, Y.; Hosono, H. High Electron Density on Ru in Intermetallic YRu2: The Application to Catalyst for Ammonia Synthesis. *J. Phys. Chem. C* **2018**, *122* (19), 10468–10475. https://doi.org/10.1021/acs.jpcc.8b02128.

(9) Hattori, M.; Iijima, S.; Nakao, T.; Hosono, H.; Hara, M. Solid Solution for Catalytic Ammonia Synthesis from Nitrogen and Hydrogen Gases at 50 °C. *Nat. Commun.* **2020**, *11* (1), 2001. https://doi.org/10.1038/s41467-020-15868-8.

(10) Wang, Q.; Pan, J.; Guo, J.; Hansen, H. A.; Xie, H.; Jiang, L.; Hua, L.; Li, H.; Guan, Y.; Wang, P.; Gao, W.; Liu, L.; Cao, H.; Xiong, Z.; Vegge, T.; Chen, P. Ternary Ruthenium Complex Hydrides for Ammonia Synthesis via the Associative Mechanism. *Nat. Catal.* **2021**, *4* (11), 959–967. https://doi.org/10.1038/s41929-021-00698-8.

(11) Kobayashi, Y.; Tang, Y.; Kageyama, T.; Yamashita, H.; Masuda, N.; Hosokawa, S.; Kageyama, H. *Titanium-Based Hydrides as Heterogeneous Catalysts for Ammonia Synthesis*. ACS Publications. https://pubs.acs.org/doi/full/10.1021/jacs.7b08891 (accessed 2022-06-02). https://doi.org/10.1021/jacs.7b08891.

(12) Hara, M.; Kitano, M.; Hosono, H. Ru-Loaded C12A7:E– Electride as a Catalyst for Ammonia Synthesis. *ACS Catal.* **2017**, *7* (4), 2313–2324. https://doi.org/10.1021/acscatal.6b03357.

(13) Wang, P.; Chang, F.; Gao, W.; Guo, J.; Wu, G.; He, T.; Chen, P. Breaking Scaling Relations to Achieve Low-Temperature Ammonia Synthesis through LiH-Mediated Nitrogen Transfer and Hydrogenation. *Nat. Chem.* **2017**, *9* (1), 64–70. https://doi.org/10.1038/nchem.2595.

(14) Ye, T.-N.; Park, S.-W.; Lu, Y.; Li, J.; Sasase, M.; Kitano, M.; Tada, T.; Hosono, H. Vacancy-Enabled N2 Activation for Ammonia Synthesis on an Ni-Loaded Catalyst. *Nature* **2020**, *583* (7816), 391–395. https://doi.org/10.1038/s41586-020-2464-9.

(15) Kitano, M.; Inoue, Y.; Yamazaki, Y.; Hayashi, F.; Kanbara, S.; Matsuishi, S.; Yokoyama, T.; Kim, S.-W.; Hara, M.; Hosono, H. Ammonia Synthesis Using a Stable Electride as an Electron Donor and Reversible Hydrogen Store. *Nat. Chem.* **2012**, *4* (11), 934–940. https://doi.org/10.1038/nchem.1476.

(16) Nørskov, J. K.; Studt, F.; Abild-Pedersen, F.; Bligaard, T. *Fundamental Concepts in Heterogeneous Catalysis: Norskov/Fundamental Concepts in Heterogeneous Catalysis*; John Wiley & Sons, Inc: Hoboken, NJ, USA, 2014. https://doi.org/10.1002/9781118892114.

(17) Kojima, R.; Aika, K. Cobalt Molybdenum Bimetallic Nitride Catalysts for Ammonia Synthesis: Part 2. Kinetic Study. *Appl. Catal. Gen.* **2001**, *218* (1), 121–128. https://doi.org/10.1016/S0926-860X(01)00626-3.

(18) Morimoto, R.; Ogawa, T. The Microkinetics of Ammonia Synthesis: The Effect of Surface Coverage on Apparent Activation Energy and Reaction Order. May 10, 2022. https://doi.org/10.26434/chemrxiv-2022-gqq4q.

(19) Kobayashi, Y.; Kitano, M.; Kawamura, S.; Yokoyama, T.; Hosono, H. Kinetic Evidence: The Rate-Determining Step for Ammonia Synthesis over Electride-Supported Ru Catalysts Is No Longer the Nitrogen Dissociation Step. *Catal. Sci. Technol.* **2017**, *7* (1), 47–50. https://doi.org/10.1039/C6CY01962E.

(20) Abe, H.; Niwa, Y.; Kitano, M.; Inoue, Y.; Murakami, Y.; Yokoyama, T.; Hara, M.; Hosono, H. High Oxidation Tolerance of Ru Nanoparticles on 12CaO·7Al2O3 Electride. *J. Phys. Chem. C* **2016**, *120* (16), 8711–8716. https://doi.org/10.1021/acs.jpcc.6b00983.